ESC HEART FAILURE
ESC Heart Failure 2023; **10**: 762–775
Published online 23 November 2022 in Wiley Online Library (wileyonlinelibrary.com) **DOI:** 10.1002/ehf2.14233

REVIEW

Adaptive versus maladaptive right ventricular remodelling

Zvonimir A. Rako, Nils Kremer, Athiththan Yogeswaran, Manuel J. Richter and Khodr Tello*

Department of Internal Medicine, Justus Liebig University Giessen, Universities of Giessen and Marburg Lung Center (UGMLC), German Center for Lung Research (DZL), Klinikstrasse 33, 35392, Giessen, Germany

Abstract

Right ventricular (RV) function and its adaptation to increased afterload [RV–pulmonary arterial (PA) coupling] are crucial in various types of pulmonary hypertension, determining symptomatology and outcome. In the course of disease progression and increasing afterload, the right ventricle undergoes adaptive remodelling to maintain right-sided cardiac output by increasing contractility. Exhaustion of compensatory RV remodelling (RV–PA uncoupling) finally leads to maladaptation and increase of cardiac volumes, resulting in heart failure. The gold-standard measurement of RV–PA coupling is the ratio of contractility [end-systolic elastance (Ees)] to afterload [arterial elastance (Ea)] derived from RV pressure–volume loops obtained by conductance catheterization. The optimal Ees/Ea ratio is between 1.5 and 2.0. RV–PA coupling in pulmonary hypertension has considerable reserve; the Ees/Ea threshold at which uncoupling occurs is estimated to be ~0.7. As RV conductance catheterization is invasive, complex, and not widely available, multiple non-invasive echocardiographic surrogates for Ees/Ea have been investigated. One of the first described and best validated surrogates is the ratio of tricuspid annular plane systolic excursion to estimated pulmonary arterial systolic pressure (TAPSE/PASP), which has shown prognostic relevance in left-sided heart failure and precapillary pulmonary hypertension. Other RV–PA coupling surrogates have been formed by replacing TAPSE with different echocardiographic measures of RV contractility, such as peak systolic tissue velocity of the lateral tricuspid annulus (S'), RV fractional area change, speckle tracking-based RV free wall longitudinal strain and global longitudinal strain, and three-dimensional RV ejection fraction. PASP-independent surrogates have also been studied, including the ratios S'/RV end-systolic area index, RV area change/RV end-systolic area, and stroke volume/end-systolic volume. Limitations of these non-invasive surrogates include the influence of severe tricuspid regurgitation (which can cause distortion of longitudinal measurements and underestimation of PASP) and the angle dependence of TAPSE and PASP. Detection of early RV remodelling may require isolated analysis of single components of RV shortening along the radial and anteroposterior axes as well as the longitudinal axis. Multiple non-invasive methods may need to be applied depending on the level of RV dysfunction. This review explains the mechanisms of RV (mal)adaptation to its load, describes the invasive assessment of RV–PA coupling, and provides an overview of studies of non-invasive surrogate parameters, highlighting recently published works in this field. Further large-scale prospective studies including gold-standard validation are needed, as most studies to date had a retrospective, single-centre design with a small number of participants, and validation against gold-standard Ees/Ea was rarely performed.

Keywords Cardiac magnetic resonance imaging; Conductance catheterization; Echocardiography; Pulmonary hypertension; Right ventricle; Ventriculoarterial coupling

Received: 23 May 2022; Revised: 29 October 2022; Accepted: 4 November 2022
**Correspondence to: Khodr Tello, Department of Internal Medicine, Justus Liebig University Giessen, Universities of Giessen and Marburg Lung Center (UGMLC), German Center for Lung Research (DZL), Klinikstrasse 33, 35392 Giessen, Germany. Email: khodr.tello@innere.med.uni-giessen.de*
Zvonimir A. Rako and Nils Kremer contributed equally.

Introduction

Right ventricular (RV) function, characterized as adaptation to increased afterload, is decisive for the course and symptoms of any kind of pulmonary hypertension (PH).[1,2] However, with constantly increasing afterload, the adaptive response transitions to pathological maladaptive remodelling. In this article, we explain the mechanisms of RV (mal)adaptation to its load

and introduce RV–pulmonary arterial (PA) coupling as a measure of this. Because the gold-standard method for assessing RV–PA coupling is invasive and technically complex, we then give an overview of simpler, validated (mostly echocardiographic) surrogate parameters.

Mechanisms of right ventricular (mal) adaptation

The crucial haemodynamic change in PH is an increase in pulmonary vascular resistance (PVR) caused by vasoconstriction, proliferative remodelling, or occlusion of the PA vasculature. The ability of the right ventricle to adapt to the increased RV afterload—RV–PA coupling—is the primary prognostic factor in PH.[2]

RV–PA coupling is described by the quotient of contractility and afterload. Optimal coupling occurs when maximal cardiac output (CO) is transferred to the pulmonary circulation at a minimal energy cost (*Figure 1A*). The early adaptation to pressure overload is an increase in contractility (homeometric adaptation).[3] This adaptation is achieved by concentric RV hypertrophy, which is characterized by increased wall thickness (cardiomyocyte hypertrophy) with almost no change in chamber volume (*Figure 1B*). Thus, force generation is increased and wall tension is reduced by an increased mass-to-volume ratio. In this adaptive state, RV–PA coupling, CO, ejection fraction (EF), and exercise capacity are maintained.

The progression of PH eventually exhausts homeometric adaptation: Contractility fails to match afterload, uncoupling occurs, and the right ventricle transitions to a maladaptive phenotype (*Figure 1C*). With sustained pressure overload, the growth of cardiomyocytes becomes limited. To preserve stroke volume (SV) and CO, the right ventricle dilates, resulting in increased wall tension, cardiomyocyte stress, and impairment of RV function. Myocyte stress and increased wall tension result in myocardial stiffening attributed to interstitial fibrosis and cardiomyocyte stiffening.[4] Adaptive RV interstitial fibrosis is a mechanism to prevent myocardial overstretching; it promotes the transfer of increasing contractile forces and supports the ventricular shape. In the maladaptive state, interstitial fibrosis leads to augmented

Figure 1 Illustration of three stages of RV remodelling in the course of progressing PH: (A) normal RV–pulmonary arterial coupling, (B) homeometric adaptation, and (C) heterometric adaptation. For further details, please see the corresponding sections of the text. Ea, arterial elastance; Ees, end-systolic elastance; IVC, inferior vena cava; PH, pulmonary hypertension; PVR, pulmonary vascular resistance; RV, right ventricular; SVC, superior vena cava.

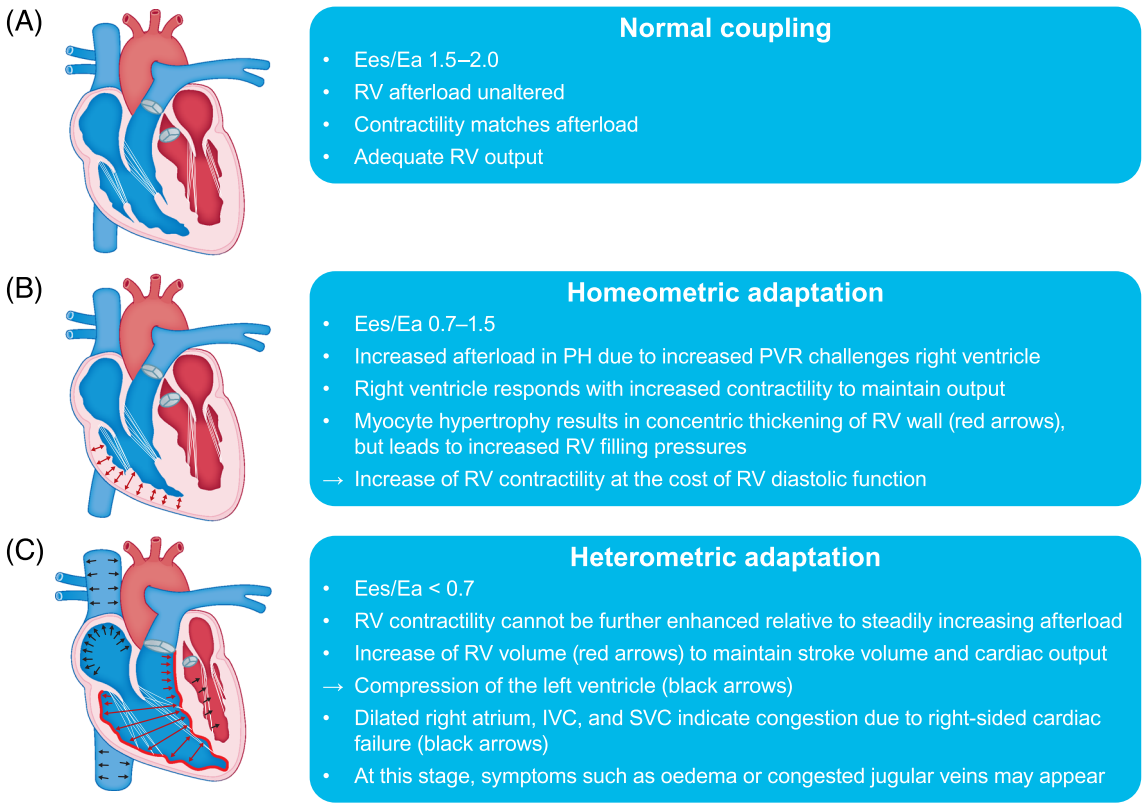

stiffness and impaired excitation–contraction coupling and cardiac contraction coordination.[5] Cardiomyocyte stiffening is primarily determined by the sarcomeric protein titin, whose compliance is regulated by phosphorylation.[4] Reduced titin phosphorylation has been shown in RV tissue from patients with pulmonary arterial hypertension (PAH).[4] In end-stage RV failure, experimental data suggest a larger contribution of interstitial fibrosis to total stiffness, whereas cardiomyocyte stiffening may play a larger role in earlier stages.[6] Both fibrosis and cardiomyocyte stiffening are associated with impaired diastolic filling and drive diastolic dysfunction, resulting in increased filling pressures and venous congestion. Mismatch of oxygen supply and demand in the maladaptive ventricle also contribute to the deterioration of RV function. Oxygen consumption is determined by wall tension,[7] which increases in the dilating ventricle. Conversely, systolic coronary flow is decreased proportional to RV mass and pressure in patients with PH and RV maladaptation[8]; capillary density is also decreased in these patients.[9] Ultimately, clinically apparent RV failure occurs, with decreased SV and EF due to inadequate contractility and diastolic filling, leading to left ventricular (LV) underfilling and haemodynamic instability.

Invasive assessment of right ventricular–pulmonary arterial coupling

To assess diastolic and systolic function and RV–PA coupling, contractility and load must be measured independently of one another, because contractility is directly related to afterload and preload. The gold standard for load-independent assessment of contractility and afterload is the analysis of pressure–volume (PV) loops, which are created by plotting ventricular pressure against ventricular volume[10] (*Figure 2*). Conductance catheters, which enable high-resolution simultaneous recording of RV pressure and volume, are the gold standard for recording PV loops. The change in volume is measured via the change in conductivity within an electric field built up between the catheter electrodes. Afterload, RV–PA coupling, and RV systolic and diastolic function are evaluated as described below.

RV systolic function (contractility) is assessed as end-systolic elastance (Ees). Ees is measured by recording multiple PV loops while reducing preload[11] (*Figure 3*). Preload reduction can be achieved by inflating a balloon in the inferior vena cava or by a Valsalva manoeuvre. The slope of the straight line through the end-systolic pressure (ESP) of each individual loop defines Ees. To avoid the complex and potentially harmful manoeuvres of preload reduction, methods were developed to assess contractility from a single beat. The single-beat method depends on a maximum RV pressure calculation based on extrapolation of RV pressure curves[12] (*Figure 3*). Recent studies showed good agreement between the single- and multi-beat methods.[13,14]

Afterload is assessed as arterial elastance (Ea), calculated as the ratio of ESP and SV.

RV–PA coupling is quantified as the ratio between end-systolic and arterial elastance (Ees/Ea).

RV diastolic function and stiffness is assessed as end-diastolic elastance (Eed). Eed is the slope of the PV relationship at end-diastole under different preload conditions (e.g. during balloon occlusion of the inferior vena cava). The elastance curve is obtained by fitting an exponential curve through the diastolic PV points. To avoid complex preload

Figure 2 Schematic representations of (A) a pressure–volume loop of the right ventricle and (B) the conductance catheter positioned in the right ventricle. In the pressure–volume loop schematic, a indicates the closure of the tricuspid valve and end of diastole (shown in green), b indicates the opening of the pulmonary valve and end of the isovolumetric contraction (1), c indicates the closure of the pulmonary valve and end of the ejection phase (2) and systole (shown in orange), and d indicates the opening of the tricuspid valve, end of isovolumetric relaxation (3), and beginning of the filling phase (4). EDP, end-diastolic pressure; EDV, end-diastolic volume; ESP, end-systolic pressure; ESV, end-systolic volume; SV, stroke volume.

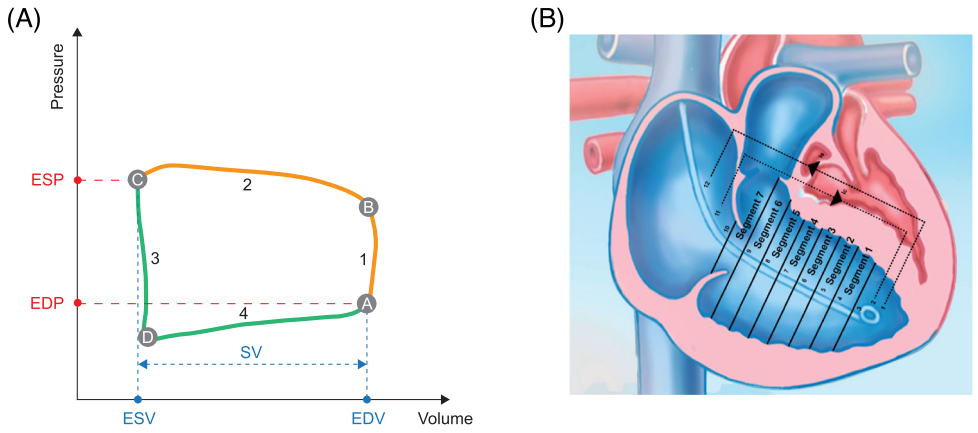

Figure 3 Determination of Ees using (A) the multi-beat method and (B) the single-beat method. In the multi-beat method, the preload is reduced from right to left and the red arrow represents Ees. In the single-beat method, Pmax is a theoretical value that represents the maximum pressure that could be reached in the right ventricle if the pulmonary valves were closed (i.e. maximum afterload). Pmax is calculated by fitting a sine function, a + b*sin (c*x + d), to the phase of isovolumetric contraction and relaxation of the pressure curve. Ees, end-systolic elastance; ESP, end-systolic pressure; Pmax, theoretical isovolumetric maximum pressure; SV, stroke volume.

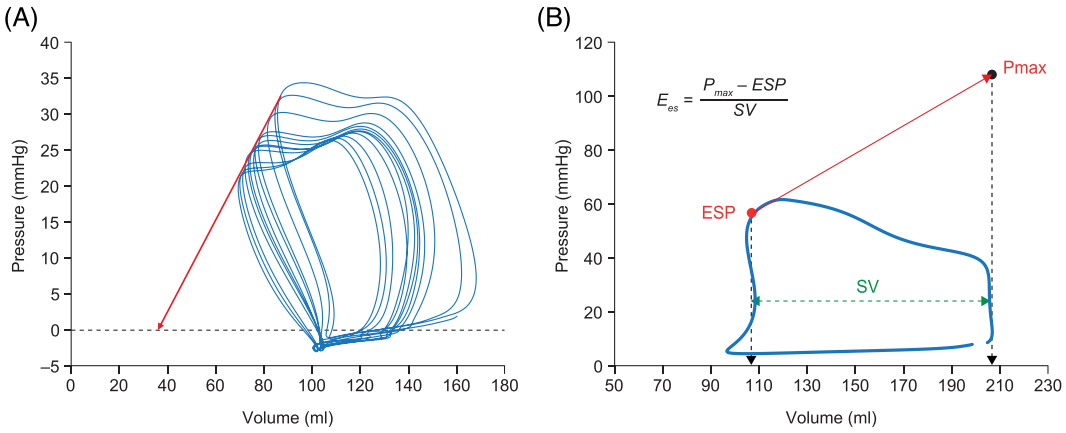

reduction manoeuvres, a single-beat method has also been developed.[4]

The optimal Ees/Ea ratio, defined as the best ratio of right-sided CO to energy input, is between 1.5 and 2.0.[1,15] However, the exact Ees/Ea threshold at which decoupling occurs is not precisely known. Axell *et al*. defined the Ees/Ea threshold below which RV dysfunction occurs as 0.68 in an animal model.[16] Similar values have been found in clinical studies: Richter *et al*. reported Ees/Ea < 0.7 as an independent predictor of clinical worsening[14]; Hsu *et al*. showed that Ees/Ea < 0.65 predicts a shorter time to clinical deterioration[17]; and Schmeisser *et al*. recently described an association of Ees/Ea ≥ 0.68 with preserved RV function and mid-term survival in patients with secondary PH due to heart failure (HF).[18] Consequently, it can be assumed that RV–PA coupling in PH has considerable reserve. Ees/Ea must decrease from normal values of 1.5 to 2 to around 0.7 before heterometric adaptation occurs, end-diastolic volume increases, and RVEF decreases below the critical value of 35%, which has been validated as a predictor of poor outcome in PH.[19–21]

Although several studies in patients with severe PH have shown that coupling can be preserved at rest, with a two-fold to three-fold increase in Ees and an Ees/Ea ratio between 0.7 and 1.5, the functional RV reserve during exercise is not yet fully understood. Stress testing of Ees/Ea could help to uncover latent or early stages of maladaptation in patients with PH, which are not apparent at rest. Hsu *et al*. observed that RV contractile reserve is depressed in patients with PAH associated with systemic sclerosis, resulting in uncoupling and acute RV dilation during exercise.[22] A more recent study used fluid challenge as an alternative to physical exercise testing.[23] Fluid challenge led to RV–PA uncoupling (inappropriate Ees and Ees/Ea values) in the majority of patients with PH, whereas controls remained coupled. The extent of RV–PA uncoupling after fluid challenge was strongly correlated with pulmonary haemodynamics at rest. The RVEF cut-off for prediction of uncoupling after fluid challenge was 48%, which is remarkably higher than the previously reported 35% at rest.

Increased Eed is significantly associated with outcome in PH and is closely associated with Ees.[24,25] However, cut-off values indicating maladapted diastolic stiffness are scarce. Trip and colleagues observed an association between Eed > 0.53 mmHg/mL and worse prognosis.[24] In another cohort, the Eed cut-off for inappropriate diastolic stiffness was 0.124 mmHg/mL.[26] Therefore, it remains unclear which Eed values indicate RV maladaptation.

Non-invasive surrogates of right ventricular–pulmonary arterial coupling

Although RV conductance catheterization is the gold standard for assessment of RV–PA coupling, it is rarely applied, as it is invasive, demanding, time-consuming, expensive, and not broadly available, and requires experience in administration and interpretation of the complex data.[27–29] Therefore, multiple non-invasive echocardiographic surrogates for Ees/Ea have been investigated. One of the first described and best validated non-invasive Doppler echocardiography-derived RV–PA coupling surrogates is the ratio of tricuspid annular plane systolic excursion and estimated pulmonary arterial systolic pressure (TAPSE/PASP) (*Figure 4*). Its 'length–force relationship' in the RV contractile cycle and its prognostic

Figure 4 Echocardiographic estimation of right ventricular (RV)–pulmonary arterial coupling. (A) Schematic of M-mode-derived tricuspid annular plane systolic excursion. (B) Schematic of peak systolic velocity of lateral tricuspid annulus (S'). (C) RV fractional area change is the planimetric percentage change of RV end-diastolic (blue) to end-systolic (red) area. (D, E) Schematics of speckle tracking-based strain measurement: percentage of (D) whole RV and (E) RV free wall shortening. (F) Three-dimensional RV volumetry. (G, H) Echocardiographic estimation of pulmonary arterial systolic pressure, based on (G) translation of peak tricuspid regurgitant velocity into trans-tricuspid pressure gradient by modified Bernoulli equation and (H) addition of central venous pressure estimated from inferior vena cava diameter and respiratory alteration of inferior vena cava diameter.

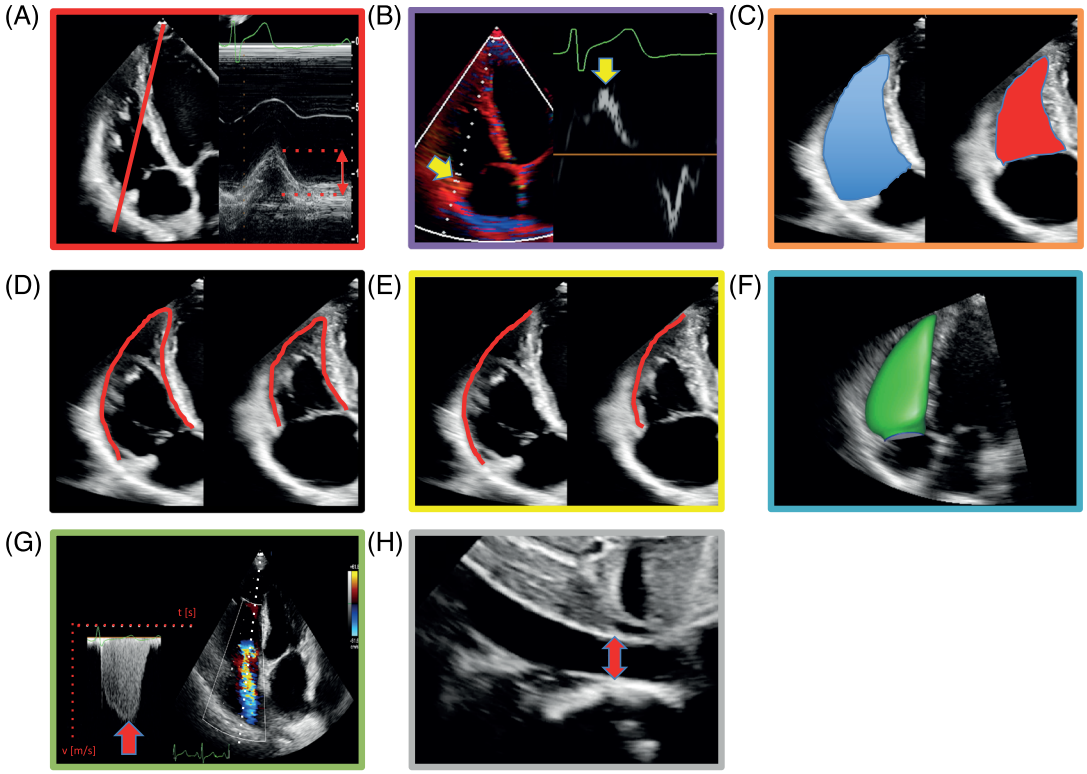

relevance were first described in the context of left-sided HF.[30] TAPSE/PASP was then assessed in precapillary PH as a prognostic non-invasive RV–PA coupling surrogate and validated against gold-standard Ees/Ea measurements, with a cut-off of 0.31 mm/mmHg to distinguish maintained coupling from RV failure.[29,31] Other RV–PA coupling surrogates were formed by replacing TAPSE with different echocardiographic measures of RV contractility, such as peak systolic tissue velocity of the lateral tricuspid annulus (S'), RV fractional area change (RVFAC), speckle tracking-based RV free wall longitudinal strain (RVFWLS) and global longitudinal strain (RVGLS), and even three-dimensional (3D) RVEF (*Figure 4*). The following sections will discuss recent publications regarding non-invasive assessment of RV–PA coupling. The reader is referred to other reviews on this topic for further information.[10,32]

Pulmonary hypertension

A study by Yogeswaran *et al*. provided support for the prognostic utility of the TAPSE/PASP ratio.[33] The authors enrolled patients with PAH who were at intermediate risk according to the guidelines of the European Society of Cardiology/European Respiratory Society (ESC/ERS) available at the time of the study[34] and evaluated an advanced risk stratification scheme, which involved subdividing the patients into high-intermediate and low-intermediate risk groups based on 6 min walk distance and TAPSE/PASP. Intriguingly, the low risk and low-intermediate risk groups showed similar survival.[33] Recently, the 6th World Symposium on PH suggested lowering the haemodynamic definition of PH from a mean PA pressure (mPAP) cut-off value of $\geq$25 to $>$20 mmHg,[35] but adjustment of the echocardiographic screening criteria for PH [which are based on the old haemodynamic definition[34] and involve quantification of the tricuspid regurgitant gradient (TRG)] was not proposed. Gall and co-workers have addressed this issue in a recent study, showing that the ratio of TAPSE to TRG was superior to TRG alone in screening for the newly proposed haemodynamic definition of PH in a large registry cohort (n = 1264) and an external validation cohort (n = 703).[36] Ghio *et al*. examined RV–PA coupling, assessed as TAPSE/PASP, during a dobutamine stress test in patients with precapillary PH.[37] They discovered a decrease of TAPSE/PASP during dobutamine exposure,

indicating worsening of RV–PA coupling and exhausted contractile reserve. This is in agreement with the results of an exercise study by Spruijt and colleagues who used invasive PV loops to evaluate RV–PA coupling.[38]

Left-sided cardiac pathologies

Ever since TAPSE/PASP was introduced as a prognostic factor in HF, non-invasive surrogate measures of RV–PA coupling have been extensively evaluated in many left-sided cardiac pathologies. RVFWLS/PASP and RVGLS/PASP predicted cardiac resynchronization therapy (CRT) response and adverse events after CRT in HF with reduced EF (HFrEF) (sensitivity 80% and specificity 77% for both).[39] In 315 stable outpatients with chronic HF (LVEF $<$ 45%), RVFWLS/PASP and RVGLS/PASP appeared superior to TAPSE/PASP in predicting mortality.[40] In patients with HFrEF treated with sacubitril/valsartan, improvement in RV–PA coupling, indicated by TAPSE/PASP, was accompanied by improvement of right- and left-sided cardiac parameters over 12 and 24 month follow-up periods.[41] Intriguingly, in multivariable analysis, the authors found right-sided cardiac improvement to be independent of LV reverse remodelling, but associated with left atrial volume index.

In a meta-analysis of four cohort studies of patients admitted with acute HF, decreased TAPSE/PASP was found to be associated with enhanced B-lines in lung ultrasound, indicating increased severity of pulmonary congestion.[42] Interestingly, reduced TAPSE/PASP at admission predicted a restricted reduction of B-lines from admission to discharge, and increased B-line occurrence at discharge (but not on admission) was associated with worse prognosis. In another prospective study, 61 stable outpatients with HF with preserved EF (HFpEF) underwent lung ultrasound, echocardiography, and right heart catheterization (RHC) at rest and during exercise.[43] Those who showed augmentation of B-lines under exercise also had reduced RV–PA coupling at rest, as indicated by TAPSE/mPAP, S′/mPAP, and RVFAC/mPAP, whereas those without an exercise-induced increase of B-lines had maintained RV–PA coupling at rest. Interestingly, no difference was found between the two subgroups regarding LV systolic and diastolic function, but left atrial function was impaired in the subgroup with exercise-induced worsening of pulmonary congestion. The authors discussed two components leading to exercise-induced pulmonary congestion: (i) Left-sided HF leads to increased PA wedge pressure and consequently increased fluid filtration of the pulmonary microvessels; (ii) right-sided HF (defined by RV–PA uncoupling) results in increased central venous pressure, which blunts pulmonary drainage of lymph.[43]

Keranov *et al*. examined TAPSE/PASP in comparison with cardiac magnetic resonance imaging (cMRI) in ischaemic and non-ischaemic cardiomyopathy and found that TAPSE/PASP $<$ 0.38 mm/mmHg predicted poor prognosis and maladaptation (indicated by increased dimensions and reduced EF and strain values) in both the right and left ventricles.[44] Low TAPSE/PASP was associated with increased T1 relaxation time at the RV insertion point, indicating fibrotic alterations.

Decreased TAPSE/PASP was also found in patients with untreated mild-to-moderate systemic hypertension compared with healthy controls, especially among male participants.[45] In 2019, Sultan *et al*. retrospectively analysed patients with severe aortic stenosis undergoing transcatheter aortic valve replacement (TAVI) and found that TAPSE/PASP was associated with post-interventional all-cause mortality.[46] A prospective single-centre cohort study of patients with severe aortic stenosis revealed improvement of RV–PA coupling (defined as S′/PASP) after TAVI, but patients with remaining RV dysfunction had persistent residual symptoms.[47]

In a retrospective study of 228 patients who underwent MitraClip application for severe mitral regurgitation, TAPSE/PASP below the median value ($\leq$0.35 mm/mmHg) was associated with post-interventional combined endpoint events, namely, HF-associated readmission and all-cause mortality.[48] RVFWLS/PASP $\leq$ 0.5%/mmHg predicted adverse outcomes over a 2 year follow-up period in patients with HF and severe secondary mitral regurgitation, regardless of treatment (MitraClip or exclusive medical treatment).[49] Fortuni *et al*. retrospectively assessed TAPSE/PASP in 1149 patients with moderate-to-severe secondary tricuspid regurgitation (TR).[50] TAPSE/PASP $<$ 0.31 mm/mmHg was associated with enlarged right and left ventricles, higher grade of TR, more pronounced HF-related symptoms, and decreased 1 and 5 year survival.

In the setting of heart transplantation, optimized donor–recipient size matching (based on predicted heart mass calculation) was associated with the largest post-transplant improvement in RV–PA coupling, as indicated by RVFAC/PASP.[51]

Schmeisser and co-workers found no benefit in indexing TAPSE by PASP compared with using TAPSE alone to assess RV–PA coupling in HFrEF, as TAPSE alone showed better correlation with Ees/Ea.[52] The same applied for RVFAC alone compared with RVFAC/PASP. The authors suggested that TAPSE alone is a measure of RV–PA coupling rather than RV contractility. Comparing their findings with those of Tello *et al*. (who identified TAPSE/PASP as an independent predictor of Ees/Ea in precapillary PH),[29] the authors assumed involvement of different pathophysiologic mechanisms in precapillary PH compared with PH due to left heart disease.

Paediatrics and congenital heart disease

Echocardiography-derived RV–PA coupling surrogates also gathered interest in the paediatric field, particularly owing to their non-invasive nature. Forton and colleagues observed an age-related decrease of TAPSE/PASP and S′/PASP from

adolescence to early adulthood in healthy volunteers.[53] In patients with atrial septal defect (ASD), initial TAPSE/PASP was shown to predict remaining symptoms after ASD closure, along with PVR index.[54] Additionally, TAPSE/PASP significantly improved after ASD closure in symptom-free patients, but not in patients with residual symptoms. Egbe *et al*. found TAPSE/PASP and RVFAC/PASP to correlate with exercise capacity (peak oxygen uptake) and occurrence of relevant arrhythmias in tetralogy of Fallot and pulmonary stenosis with pulmonary regurgitation, consequently reflecting disease severity.[55]

Intensive care medicine

RV–PA coupling has been studied in intensive care medicine recently, with promising findings. Kim and colleagues found that S'/PASP, TAPSE/PASP, and RVFWLS/PASP outperformed conventional left-sided cardiac parameters for the prediction of successful weaning from veno-arterial extracorporeal membrane oxygenation (ECMO), with S'/PASP showing the best predictive ability.[56] Unfortunately, very few patients underwent invasive haemodynamic analysis by RHC, and PV loop-derived Ees/Ea was not obtained. A retrospective study by Bleakley *et al*. showed that RVFAC was more impaired than strictly longitudinal parameters such as TAPSE, S', or RVFWLS in 90 patients with COVID-19 acute respiratory distress syndrome undergoing mechanical ventilation (38 with veno-venous ECMO), indicating impairment of RV radial function rather than longitudinal function.[57] RV–PA coupling, as indicated by RVFAC/PASP, correlated with PVR and alanine aminotransferase levels, indicating hepatic congestion in RV–PA uncoupling.

Right ventricular–pulmonary arterial coupling in other disease entities

Non-invasive RV–PA coupling assessment was also performed in other disease entities beyond those focused on the cardiopulmonary unit. In a case–control study, patients with rheumatoid arthritis showed significantly lower TAPSE/PASP than matched controls,[58] but no participant had TAPSE/PASP below a threshold of 0.36 mm/mmHg. The prognostic value of TAPSE/PASP was not assessed. Intriguingly, van Wezenbeek and co-workers recently found altered expression of sex hormones in PAH to be potentially associated with disease severity and outcome.[59] The authors described a potential role for increased androgen levels in promoting RV functional impairment. Further research is potentially worthwhile in this field. The prognostic relevance of TAPSE/PASP regarding all-cause mortality was demonstrated recently in a multicentre study including 444 patients with TR who underwent transcatheter tricuspid valve replacement or repair.[60]

Pulmonary arterial systolic pressure-independent right ventricular–pulmonary arterial coupling surrogates

TR is not always detectable in echocardiography, especially in patients without signs of PH; this may lead to exclusion from studies and selection bias, as PASP cannot be estimated. Alternative surrogate measures of RV–PA coupling excluding PASP have therefore been developed. Boulate and co-workers validated the ratio of S' to RV end-systolic area index (S'/RVESAi) against Ees/Ea in a piglet model of chronic thromboembolic PH.[61] S'/RVESAi correlated well with Ees/Ea regarding both absolute values after volume challenge (R^2 = 0.69, $P < 0.001$) and changes after haemodynamic stabilization with dobutamine (R^2 = 0.64, $P < 0.001$). S'/RVESAi also predicted adverse outcome in two cohorts of patients with PAH (stable vs. acutely decompensated). However, S'/RVESAi has not yet been validated against gold-standard Ees/Ea in humans. RV–PA coupling was impaired in a cohort of patients with repaired tetralogy of Fallot compared with controls, as indicated by S'/RVESAi and RV area change (RVAC)/RVESA.[62] Previously, RVAC/RVESA was shown to correlate with gold-standard Ees/Ea in precapillary PH[29] (see also *Table 1*).

Non-invasive 3D assessment of right ventricular–pulmonary arterial coupling

Two-dimensional echocardiography is commonly applied in the assessment of RV function in PH, but owing to the complex asymmetrical crescent-like RV anatomy with prominent trabeculae, it is logically not able to capture the entire right ventricle.[64,65] Unlike common echocardiography, 3D echocardiography captures the entire right ventricle, including the RV outflow tract region.[64,65] Although it tends to underestimate volumes compared with gold-standard cMRI, 3D echocardiography is able to accurately illustrate dimensional and functional relationships.[66,67] This provides a rationale for the use of 3D imaging parameters in surrogate measures of RV–PA coupling.

Previously, the cMRI-derived ratio of SV and end-systolic volume (SV/ESV) was shown to independently predict survival as a non-invasive measure of RV–PA coupling in 50 patients evaluated for suspected PH.[25] Presuming that Ees = ESP/ESV and Ea = ESP/SV, the combination of both equations results in Ees/Ea = SV/ESV.[68] Richter *et al*. demonstrated a good and highly significant correlation between SV/ESV and gold-standard Ees/Ea.[14] Aubert *et al*. found a good correlation between 3D echocardiography-derived SV/ESV and RV–PA coupling measured by a combination of cMRI and RHC in 90 patients with suspected PH and 30 healthy controls.[69] Similarly, paediatric patients with PH showed lower 3D SV/ESV than controls in a retrospective study[68];

Table 1 Comparison of features of different echocardiographic modalities

	TAPSE	S′	RVFAC	RV strain	3D RV volumetry
Angulation	Angle dependent[87–89]	Angle dependent[87,89]	Independent of angulation	Independent of angulation[73,88–90]	Independent of angulation
Application	Simple and reproducible[89]	Simple and reproducible	Complex; correct tracking of RV endocardial border required	Complex; correct endocardial tracking required[88,89]	Complex; precise imaging with adequate frame rate required
RV regions covered	Basal free wall and lateral tricuspid valve insertion[40]	Basal free wall[87]	Entire RV section in apical 4-chamber view	Global and regional analysis of 6 segments[40]	All RV regions; accounts for complex RV anatomy
Shortening axis	Longitudinal[64,75]	Longitudinal[64,75]	Longitudinal and radial[64,73,75]	Longitudinal[64]	Longitudinal, radial, and anteroposterior

3D, three-dimensional; RV, right ventricular; RVFAC, right ventricular fractional area change; TAPSE, tricuspid annular plane systolic excursion.

SV/ESV decreased with increasing disease severity and predicted adverse outcome. However, SV/ESV neglects RV volume at zero pressure (V_0) and sets it at 0 mL, which might be misleading because V_0 was shown to correlate with ESV.[27,70]

In a multicentre cohort of elderly individuals, 3D RVEF/PASP was found to be impaired with progressing stage of HF.[71] Intriguingly, worse 3D RVEF/PASP was associated with an increased risk of death and incident HF in participants without apparent HF. In 60 prospectively enrolled stable outpatients with non-ischaemic dilated cardiomyopathy, Vijiiac *et al*. showed that RVFWLS/PASP and 3D RVEF/PASP (but not SV/ESV) independently predicted HF-associated hospitalization.[72] However, Ishiwata *et al*. concluded that indexing RV functional parameters to PASP did not improve prognostic ability in their dilated cardiomyopathy cohort.[73] Instead, they found a combination of RVFAC and RVFWLS to improve prediction of outcome, as RVFAC covers longitudinal and radial RV shortening and RVFWLS is independent of angulation. Li and co-workers retrospectively examined 3D RVEF/PASP in precapillary PH.[63] They described a predictive value regarding adverse events, but gold-standard validation against Ees/Ea is still lacking. Richter and co-workers developed a non-invasive approach to deduce RV PV loops[27]: RV 3D echocardiography was applied to obtain a volume–time (Vt) curve, whereas a pressure–time (Pt) curve was provided by a reference curve, which was fitted according to Doppler echocardiography-derived PASP, RV outflow tract profile, and electrocardiography. Vt and Pt curves were synchronized to form PV loops. Non-invasive PV loop-derived Ees and Ees/Ea showed good correlations with gold-standard parameters, potentially providing a promising alternative to RV conductance catheterization.

Isolated analysis of single components of RV shortening along the longitudinal, radial, and anteroposterior axes can be achieved using 3D echocardiography.[65,74–76] In left-sided heart disease with mild-to-moderate LVEF impairment, Surkova and co-workers found that 3D RVEF was maintained, but isolated components of RV shortening were altered in a distinct pattern, indicating adaptive remodelling.[76] Early remodelling may therefore be overlooked using 3D RVEF only, as it may initially remain maintained despite ongoing RV remodelling and does not distinguish between longitudinal, radial, and anteroposterior deformation, as demonstrated by Surkova and co-workers.[76] Interestingly, anteroposterior shortening, which is not captured by conventional two-dimensional echocardiographic RV functional parameters,[75] had a higher area under the receiver operating characteristic curve than other RV functional parameters and was shown to independently predict adverse outcome in patients with left-sided heart disease.[76] Similarly, patients with corrected transposition of the great arteries showed differing contraction patterns compared with healthy controls.[75]

Left ventricular–right ventricular asynchrony, timing of right ventricular contraction, and right ventricular myocardial work

Apart from non-invasive RV–PA coupling surrogates, which describe the extent of RV shortening, the timing of RV shortening plays an important role in the assessment of RV maladaptation. Marcus and colleagues described the underlying mechanism of RV–LV asynchrony in PAH.[77] In PAH, delayed peak systolic shortening in the right ventricle compared with the left ventricle is caused by post-systolic RV shortening, promoting septal bowing in LV early diastole and consequently impairment of LV diastolic filling and SV. Intriguingly, the onset of RV and LV contraction did not differ, which is why the authors attributed leftward ventricular septal bowing to increased RV wall tension instead of asynchronous electrical conduction. Correspondingly, Lumens and co-workers assessed early diastolic LV lengthening [LV early diastolic strain index (LVEDSI); the portion of diastolic LV free wall lengthening during the time period between LV and RV peak systolic shortening in relation to total LV

shortening] in chronic PH.[78] LVEDSI was more pronounced in patients with PH than in controls and correlated with RV function, as indicated by cMRI and RHC. Badagliacca *et al*. assessed post-systolic RV strain curves in patients with idiopathic PAH and found three patterns[79]: a rapid return to baseline after peak systolic strain (also seen in healthy controls); a plateau in early diastole at the level of peak systolic strain before an end-diastolic return to baseline; and a decelerated return to baseline during diastole. These findings were associated with haemodynamic indices and may provide further and more accurate information to the examiner than conventional parameters. Prolonged post-systolic RV contraction and interventricular asynchrony regarding time of peak shortening result in insufficient isovolumetric RV contraction against a closed pulmonary valve, whereas the left ventricle is already in early diastole, resulting in leftward septal bowing and consequently LV diastolic impairment.[78,80]

Initially introduced for the left ventricle,[81] myocardial work (MW) was successfully transferred to the right ventricle by Butcher *et al*., who also revealed superiority of the method compared with common echocardiographic parameters in estimating invasively assessed RV stroke work index and PVR.[82,83] Non-invasive quantification of RVMW from pressure–strain loops [constructed from RV strain, pulmonary pressures (determined invasively or non-invasively), and valvular events] incorporates contractility, afterload, RV dyssynchrony, and post-systolic shortening in the RV functional assessment.[83,84] It provides indices such as RV constructive work, wasted work, work index, and work efficiency and is consequently able to quantify the portion of MW that actually contributes to RV output and the share that does not, such as post-systolic shortening. RVMW index was the only parameter found to detect graft failure-related transition from RV adaptation to failure in heart transplant recipients.[84] The integration of RV contractility and afterload mean that RVMW may also be regarded as a measure of RV–PA coupling.[83]

Summary

Outcome and symptomatology are closely related to RV–PA coupling in various diseases,[2,85,86] but gold-standard Ees/Ea is not broadly available and mainly restricted to expert centres[27–29]; there is therefore substantial demand for alternative, preferably non-invasive methods, as demonstrated by the numerous recent publications in this field. Still, the findings must be interpreted with caution.

RV–PA coupling surrogates such as TAPSE/PASP have gained high interest in the recent past, certainly owing to their non-invasive nature and easy acquisition. However, their reliability in clinical use remains debatable, and the examiner should be aware of the limitations of the parameters applied (see *Table 2*). For instance, strictly longitudinal parameters are load dependent, and measurements may be distorted in the case of pronounced TR owing to retrograde unloading into the right atrium.[63,84] Severe TR may lead to underestimation of PASP.[34] In highly advanced PH stages, PASP decreases with RV failure,[91] potentially promoting misinterpretation as mild PH. Both TAPSE and PASP are angle dependent and may be prone to erroneous quantification.[87–89] Although Doppler-derived PASP was shown to be a good PH screening parameter (a PASP threshold of >36 mmHg had 87% sensitivity and 79% specificity[92]), it lacks precision when compared with PASP invasively determined by RHC.[93,94] Both overestimation of TAPSE and underestimation of PASP favour augmentation and pseudo-normalization of TAPSE/PASP. Finally, one should also be aware of the dependence of echocardiographic parameters on the scale of RV dysfunction. Consequently, RV function should not be assessed based on a single parameter but on multiple methods, which may be reasonably applied depending on the level of RV dysfunction, as recently recommended by Sade and Katz.[95] Especially in advanced stages of RV impairment, which are accompanied by RV chamber and tricuspid annular dilatation, TAPSE might be overestimated in the presence of severe TR.[96] Additionally, TR is associated with overestimation of PASP.[97] The best

Table 2 Examples of right ventricular–pulmonary arterial coupling surrogate parameters and cut-off values for prediction of events

Prediction of event	Parameter	Cut-off value
Uncoupling measured by gold-standard Ees/Ea in patients with PAH[29]	TAPSE/PASP	<0.31 mm/mmHg
Mortality during follow-up after significant secondary tricuspid regurgitation diagnosis[50]	TAPSE/PASP	<0.31 mm/mmHg
Mortality in patients with heart failure[30]	TAPSE/PASP	<0.36 mm/mmHg
Transplant-free survival in patients with PH[25]	SV/ESV	>0.515
Adverse outcomes in patients with precapillary PH[63]	RVEF/PASP	<0.44%/mmHg
Response to CRT[39a]	RVGLS/PASP	>0.35%/mmHg
	RVFWLS/PASP	>0.41%/mmHg
12 month mortality in outpatients with stable heart failure[40a]	RVGLS/PASP	<0.36%/mmHg
	RVFWLS/PASP	<0.65%/mmHg
Poor prognosis and RV/LV maladaptation[44]	TAPSE/PASP	<0.38 mm/mmHg

CRT, cardiac resynchronization therapy; Ea, arterial elastance; Ees, end-systolic elastance; ESV, end-systolic volume; LV, left ventricular; PAH, pulmonary arterial hypertension; PASP, pulmonary arterial systolic pressure; PH, pulmonary hypertension; RV, right ventricular; RVEF, right ventricular ejection fraction; RVFWLS, right ventricular free wall longitudinal strain; RVGLS, right ventricular global longitudinal strain; SV, stroke volume; TAPSE, tricuspid annular plane systolic excursion.
[a]Authors excluded minus sign for strain.

understanding of RV function is certainly gained by quantifying RV–PA coupling, as it reflects the adequacy of contractility adaptation to afterload. 3D echocardiography-derived SV/ESV might be of particular importance at this juncture, especially in advanced RV dysfunction, because no estimation of pressures is involved.

Still, TAPSE/PASP is one of the few coupling surrogates with validation against gold-standard PV loop-derived Ees/Ea,[14,29] and its impact as a prognostic marker has been demonstrated in studies with larger cohorts.[31,36,60] Just recently, the 2022 ESC/ERS guidelines for the diagnosis and treatment of PH were published, now including TAPSE/PASP as an echocardiographic parameter for risk assessment.[98]

The right ventricle is a complex crescent-like 3D structure and demonstrates shortening along three spatial axes,[65,74] which are not captured by exclusively longitudinal functional parameters. The importance of non-longitudinal RV shortening has been repeatedly demonstrated.[75,84,99] The entire right ventricle is included in 3D echocardiography, but only isolated analysis of shortening components may detect early remodelling.[76] All in all, a combination of several parameters may yield better RV assessment than a single measure.[73]

Most of the studies had a retrospective, single-centre design with small numbers of participants. Also, validation against gold-standard Ees/Ea was rarely performed. To the best of our knowledge, only TAPSE/PASP and RVFAC/PASP were successfully validated against Ees/Ea.[29,52] Consequently, there remains a need for further large-scale prospective studies, including gold-standard validation.

Non-invasive assessment of diastolic RV function may gain importance in the future, as it is closely related to outcome in PH.[24] Wessels *et al*. recently demonstrated that RV diastolic impairment alters right atrial (RA) function in PAH.[100] Thus, non-invasive measurement of RA parameters for PH risk stratification[34] somewhat embodies assessment of RV diastolic function, as suggested by the authors.[100] However, RA impairment and RA pressure increase may not always be the consequence of RV dysfunction per se and must be evaluated in the context of the underlying disease, as recently shown by van Wezenbeek *et al*., comparing PAH and PH in HFpEF at matched levels of pressure overload.[101] Consequently, simple non-invasive surrogates of RV diastolic function are sought and may attract attention in the near future.

Acknowledgements

Editorial assistance was provided by Claire Mulligan, PhD (Beacon Medical Communications Ltd, Brighton, UK), funded by the University of Giessen.

Open Access funding enabled and organized by Projekt DEAL.

Conflict of interest

Dr Rako and Mr Kremer declare that they have no relationships relevant to the contents of this article to disclose. Dr Yogeswaran has received speaker honoraria from MSD. Dr Richter has received research support from United Therapeutics and Bayer; speaker honoraria from Bayer, Actelion, Mundipharma, Roche, and OMT; and consultancy fees from Bayer. Dr Tello has received speaker honoraria from Actelion and Bayer.

Funding

This review article was supported by the Deutsche Forschungsgemeinschaft under Grant Agreement No. CRC1213, Project B08. Open Access funding was enabled and organized by Projekt DEAL (WOA Institution: Justus Liebig Universitaet Giessen; Consortia Name: Projekt DEAL).

References

1. Lahm T, Douglas IS, Archer SL, Bogaard HJ, Chesler NC, Haddad F, Hemnes AR, Kawut SM, Kline JA, Kolb TM, Mathai SC, Mercier O, Michelakis ED, Naeije R, Tuder RM, Ventetuolo CE, Vieillard-Baron A, Voelkel NF, Vonk-Noordegraaf A, Hassoun PM, American Thoracic Society Assembly on Pulmonary Circulation. Assessment of right ventricular function in the research setting: knowledge gaps and pathways forward. An official American Thoracic Society research statement. *Am J Respir Crit Care Med*. 2018; **198**: e15–e43.
2. Vonk Noordegraaf A, Chin KM, Haddad F, Hassoun PM, Hemnes AR, Hopkins SR, Kawut SM, Langleben D, Lumens J, Naeije R. Pathophysiology of the right ventricle and of the pulmonary circulation in pulmonary hypertension: an update. *Eur Respir J*. 2019; **53**: 1801900.
3. Vieillard-Baron A, Naeije R, Haddad F, Bogaard HJ, Bull TM, Fletcher N, Lahm T, Magder S, Orde S, Schmidt G, Pinsky MR. Diagnostic workup, etiologies and management of acute right ventricle failure: a state-of-the-art paper. *Intensive Care Med*. 2018; **44**: 774–790.
4. Rain S, Handoko ML, Trip P, Gan CT, Westerhof N, Stienen GJ, Paulus WJ, Ottenheijm CA, Marcus JT, Dorfmuller P, Guignabert C, Humbert M, Macdonald P, Dos Remedios C, Postmus PE, Saripalli C, Hidalgo CG, Granzier HL, Vonk-Noordegraaf A, van der Velden J, de Man FS. Right ventricular diastolic impairment in patients with pulmonary arterial hypertension. *Circulation*. 2013; **128**: 2016–2025.
5. Andersen S, Nielsen-Kudsk JE, Vonk Noordegraaf A, de Man FS. Right

ventricular fibrosis. *Circulation*. 2019; **139**: 269–285.
6. Rain S, Andersen S, Najafi A, Gammelgaard Schultz J, da Silva Goncalves Bos D, Handoko ML, Bogaard HJ, Vonk-Noordegraaf A, Andersen A, van der Velden J, Ottenheijm CA, de Man FS. Right ventricular myocardial stiffness in experimental pulmonary arterial hypertension: relative contribution of fibrosis and myofibril stiffness. *Circ Heart Fail*. 2016; **9**: e002636.
7. Sarnoff SJ, Braunwald E, Welch GH Jr, Case RB, Stainsby WN, Macruz R. Hemodynamic determinants of oxygen consumption of the heart with special reference to the tension-time index. *Am J Physiol*. 1958; **192**: 148–156.
8. van Wolferen SA, Marcus JT, Westerhof N, Spreeuwenberg MD, Marques KM, Bronzwaer JG, Henkens IR, Gan CT, Boonstra A, Postmus PE, Vonk-Noordegraaf A. Right coronary artery flow impairment in patients with pulmonary hypertension. *Eur Heart J*. 2008; **29**: 120–127.
9. Ruiter G, Ying Wong Y, de Man FS, Louis Handoko M, Jaspers RT, Postmus PE, Westerhof N, Niessen HW, van der Laarse WJ, Vonk-Noordegraaf A. Right ventricular oxygen supply parameters are decreased in human and experimental pulmonary hypertension. *J Heart Lung Transplant*. 2013; **32**: 231–240.
10. Tello K, Gall H, Richter M, Ghofrani A, Schermuly R. Right ventricular function in pulmonary (arterial) hypertension. *Herz*. 2019; **44**: 509–516.
11. Maughan WL, Shoukas AA, Sagawa K, Weisfeldt ML. Instantaneous pressure-volume relationship of the canine right ventricle. *Circ Res*. 1979; **44**: 309–315.
12. Brimioulle S, Wauthy P, Ewalenko P, Rondelet B, Vermeulen F, Kerbaul F, Naeije R. Single-beat estimation of right ventricular end-systolic pressure-volume relationship. *Am J Physiol Heart Circ Physiol*. 2003; **284**: H1625–H1630.
13. Inuzuka R, Hsu S, Tedford RJ, Senzaki H. Single-beat estimation of right ventricular contractility and its coupling to pulmonary arterial load in patients with pulmonary hypertension. *J Am Heart Assoc*. 2018; **7**: e007929.
14. Richter MJ, Peters D, Ghofrani HA, Naeije R, Roller F, Sommer N, Gall H, Grimminger F, Seeger W, Tello K. Evaluation and prognostic relevance of right ventricular-arterial coupling in pulmonary hypertension. *Am J Respir Crit Care Med*. 2020; **201**: 116–119.
15. Naeije R, Brimioulle S, Dewachter L. Biomechanics of the right ventricle in health and disease (2013 Grover Conference series). *Pulm Circ*. 2014; **4**: 395–406.
16. Axell RG, Messer SJ, White PA, McCabe C, Priest A, Statopoulou T, Drozdzynska M, Viscasillas J, Hinchy EC, Hampton-Till J, Alibhai HI, Morrell N, Pepke-Zaba J, Large SR, Hoole SP. Ventriculo-arterial coupling detects occult RV dysfunction in chronic thromboembolic pulmonary vascular disease. *Physiol Rep*. 2017; **5**: e13227.
17. Hsu S, Simpson CE, Houston BA, Wand A, Sato T, Kolb TM, Mathai SC, Kass DA, Hassoun PM, Damico RL, Tedford RJ. Multi-beat right ventricular-arterial coupling predicts clinical worsening in pulmonary arterial hypertension. *J Am Heart Assoc*. 2020; **9**: e016031.
18. Schmeisser A, Rauwolf T, Groscheck T, Fischbach K, Kropf S, Luani B, Tanev I, Hansen M, Meissler S, Schafer K, Steendijk P, Braun-Dullaeus RC. Predictors and prognosis of right ventricular function in pulmonary hypertension due to heart failure with reduced ejection fraction. *ESC Heart Fail*. 2021; **8**: 2968–2981.
19. Brewis MJ, Bellofiore A, Vanderpool RR, Chesler NC, Johnson MK, Naeije R, Peacock AJ. Imaging right ventricular function to predict outcome in pulmonary arterial hypertension. *Int J Cardiol*. 2016; **218**: 206–211.
20. van de Veerdonk MC, Kind T, Marcus JT, Mauritz GJ, Heymans MW, Bogaard HJ, Boonstra A, Marques KM, Westerhof N, Vonk-Noordegraaf A. Progressive right ventricular dysfunction in patients with pulmonary arterial hypertension responding to therapy. *J Am Coll Cardiol*. 2011; **58**: 2511–2519.
21. Vanderpool RR, Rischard F, Naeije R, Hunter K, Simon MA. Simple functional imaging of the right ventricle in pulmonary hypertension: can right ventricular ejection fraction be improved? *Int J Cardiol*. 2016; **223**: 93–94.
22. Hsu S, Houston BA, Tampakakis E, Bacher AC, Rhodes PS, Mathai SC, Damico RL, Kolb TM, Hummers LK, Shah AA, McMahan Z, Corona-Villalobos CP, Zimmerman SL, Wigley FM, Hassoun PM, Kass DA, Tedford RJ. Right ventricular functional reserve in pulmonary arterial hypertension. *Circulation*. 2016; **133**: 2413–2422.
23. Kremer N, Rako Z, Douschan P, Gall H, Ghofrani HA, Grimminger F, Guth S, Naeije R, Rieth A, Schulz R, Seeger W, Tedford RJ, Vadasz I, Vanderpool R, Wiedenroth CB, Richter MJ, Tello K. Unmasking right ventricular-arterial uncoupling during fluid challenge in pulmonary hypertension. *J Heart Lung Transplant*. 2022; **41**: 345–355.
24. Trip P, Rain S, Handoko ML, van der Bruggen C, Bogaard HJ, Marcus JT, Boonstra A, Westerhof N, Vonk-Noordegraaf A, de Man FS. Clinical relevance of right ventricular diastolic stiffness in pulmonary hypertension. *Eur Respir J*. 2015; **45**: 1603–1612.
25. Vanderpool RR, Pinsky MR, Naeije R, Deible C, Kosaraju V, Bunner C, Mathier MA, Lacomis J, Champion HC, Simon MA. RV-pulmonary arterial coupling predicts outcome in patients referred for pulmonary hypertension. *Heart*. 2015; **101**: 37–43.
26. Tello K, Dalmer A, Vanderpool R, Ghofrani HA, Naeije R, Roller F, Seeger W, Wilhelm J, Gall H, Richter MJ. Cardiac magnetic resonance imaging-based right ventricular strain analysis for assessment of coupling and diastolic function in pulmonary hypertension. *JACC Cardiovasc Imaging*. 2019; **12**: 2155–2164.
27. Richter MJ, Yogeswaran A, Husain-Syed F, Vadasz I, Rako Z, Mohajerani E, Ghofrani HA, Naeije R, Seeger W, Herberg U, Rieth A, Tedford RJ, Grimminger F, Gall H, Tello K. A novel non-invasive and echocardiography-derived method for quantification of right ventricular pressure-volume loops. *Eur Heart J Cardiovasc Imaging*. 2022; **23**: 498–507.
28. Tello K, Dalmer A, Axmann J, Vanderpool R, Ghofrani HA, Naeije R, Roller F, Seeger W, Sommer N, Wilhelm J, Gall H, Richter MJ. Reserve of right ventricular-arterial coupling in the setting of chronic overload. *Circ Heart Fail*. 2019; **12**: e005512.
29. Tello K, Wan J, Dalmer A, Vanderpool R, Ghofrani HA, Naeije R, Roller F, Mohajerani E, Seeger W, Herberg U, Sommer N, Gall H, Richter MJ. Validation of the tricuspid annular plane systolic excursion/systolic pulmonary artery pressure ratio for the assessment of right ventricular-arterial coupling in severe pulmonary hypertension. *Circ Cardiovasc Imaging*. 2019; **12**: e009047.
30. Guazzi M, Bandera F, Pelissero G, Castelvecchio S, Menicanti L, Ghio S, Temporelli PL, Arena R. Tricuspid annular plane systolic excursion and pulmonary arterial systolic pressure relationship in heart failure: an index of right ventricular contractile function and prognosis. *Am J Physiol Heart Circ Physiol*. 2013; **305**: H1373–H1381.
31. Tello K, Axmann J, Ghofrani HA, Naeije R, Narcin N, Rieth A, Seeger W, Gall H, Richter MJ. Relevance of the TAPSE/PASP ratio in pulmonary arterial hypertension. *Int J Cardiol*. 2018; **266**: 229–235.
32. Tello K, Seeger W, Naeije R, Vanderpool R, Ghofrani HA, Richter M, Tedford RJ, Bogaard HJ. Right heart failure in pulmonary hypertension: diagnosis and new perspectives on vascular and direct right ventricular treatment. *Br J Pharmacol*. 2021; **178**: 90–107.
33. Yogeswaran A, Richter MJ, Sommer N, Ghofrani HA, Seeger W, Tello K, Gall H. Advanced risk stratification of intermediate risk group in pulmonary arterial hypertension. *Pulm Circ*. 2020; **10**: 1–5.
34. Galie N, Humbert M, Vachiery JL, Gibbs S, Lang I, Torbicki A, Simonneau G, Peacock A, Vonk Noordegraaf A,

Beghetti M, Ghofrani A, Gomez Sanchez MA, Hansmann G, Klepetko W, Lancellotti P, Matucci M, Mcdonagh T, Pierard LA, Trindade PT, Zompatori M, Hoeper M, Group ESCSD. 2015 ESC/ERS Guidelines for the diagnosis and treatment of pulmonary hypertension: the joint task force for the diagnosis and treatment of pulmonary hypertension of the European Society of Cardiology (ESC) and the European Respiratory Society (ERS): endorsed by: Association for European Paediatric and Congenital Cardiology (AEPC), International Society for Heart and Lung Transplantation (ISHLT). *Eur Heart J*. 2016; **37**: 67–119.

35. Simonneau G, Montani D, Celermajer DS, Denton CP, Gatzoulis MA, Krowka M, Williams PG, Souza R. Haemodynamic definitions and updated clinical classification of pulmonary hypertension. *Eur Respir J*. 2019; **53**: 1801913.
36. Gall H, Yogeswaran A, Fuge J, Sommer N, Grimminger F, Seeger W, Olsson KM, Hoeper MM, Richter MJ, Tello K, Ghofrani HA. Validity of echocardiographic tricuspid regurgitation gradient to screen for new definition of pulmonary hypertension. *EClinicalMedicine*. 2021; **34**: 100822.
37. Ghio S, Fortuni F, Greco A, Turco A, Lombardi C, Scelsi L, Raineri C, Matrone B, Vullo E, Guida S, Badagliacca R, Oltrona VL. Dobutamine stress echocardiography in pulmonary arterial hypertension. *Int J Cardiol*. 2018; **270**: 331–335.
38. Spruijt OA, de Man FS, Groepenhoff H, Oosterveer F, Westerhof N, Vonk-Noordegraaf A, Bogaard HJ. The effects of exercise on right ventricular contractility and right ventricular-arterial coupling in pulmonary hypertension. *Am J Respir Crit Care Med*. 2015; **191**: 1050–1057.
39. Deaconu S, Deaconu A, Scarlatescu A, Petre I, Onciul S, Vijiiac A, Zamfir D, Marascu G, Iorgulescu C, Radu AD, Bogdan S, Vatasescu R. Ratio between right ventricular longitudinal strain and pulmonary arterial systolic pressure: novel prognostic parameter in patients undergoing cardiac resynchronization therapy. *J Clin Med*. 2021; **10**: 2442.
40. Iacoviello M, Monitillo F, Citarelli G, Leone M, Grande D, Antoncecchi V, Rizzo C, Terlizzese P, Romito R, Caldarola P, Ciccone MM. Right ventriculo-arterial coupling assessed by two-dimensional strain: a new parameter of right ventricular function independently associated with prognosis in chronic heart failure patients. *Int J Cardiol*. 2017; **241**: 318–321.
41. Masarone D, Errigo V, Melillo E, Valente F, Gravino R, Verrengia M, Ammendola E, Vastarella R, Pacileo G. Effects of sacubitril/valsartan on the right ventricular arterial coupling in patients with heart failure with reduced ejection fraction. *J Clin Med*. 2020; **9**: 3159.
42. Kobayashi M, Gargani L, Palazzuoli A, Ambrosio G, Bayes-Genis A, Lupon J, Pellicori P, Pugliese NR, Reddy YNV, Ruocco G, Duarte K, Huttin O, Rossignol P, Coiro S, Girerd N. Association between right-sided cardiac function and ultrasound-based pulmonary congestion on acutely decompensated heart failure: findings from a pooled analysis of four cohort studies. *Clin Res Cardiol*. 2021; **110**: 1181–1192.
43. Reddy YNV, Obokata M, Wiley B, Koepp KE, Jorgenson CC, Egbe A, Melenovsky V, Carter RE, Borlaug BA. The haemodynamic basis of lung congestion during exercise in heart failure with preserved ejection fraction. *Eur Heart J*. 2019; **40**: 3721–3730.
44. Keranov S, Haen S, Vietheer J, Rutsatz W, Wolter JS, Kriechbaum SD, von Jeinsen B, Bauer P, Tello K, Richter M, Dorr O, Rieth AJ, Nef H, Hamm CW, Liebetrau C, Rolf A, Keller T. Application and validation of the tricuspid annular plane systolic excursion/systolic pulmonary artery pressure ratio in patients with ischemic and non-ischemic cardiomyopathy. *Diagnostics (Basel)*. 2021; **11**: 2188.
45. Vriz O, Pirisi M, Bossone E, Fadl ElMula FEM, Palatini P, Naeije R. Right ventricular-pulmonary arterial uncoupling in mild-to-moderate systemic hypertension. *J Hypertens*. 2020; **38**: 274–281.
46. Sultan I, Cardounel A, Abdelkarim I, Kilic A, Althouse AD, Sharbaugh MS, Gupta A, Xu J, Fukui M, Simon MA, Schindler JT, Lee JS, Gleason TG, Cavalcante JL. Right ventricle to pulmonary artery coupling in patients undergoing transcatheter aortic valve implantation. *Heart*. 2019; **105**: 117–121.
47. Eleid MF, Padang R, Pislaru SV, Greason KL, Crestanello J, Nkomo VT, Pellikka PA, Jentzer JC, Gulati R, Sandhu GS, Holmes DR Jr, Nishimura RA, Rihal CS, Borlaug BA. Effect of transcatheter aortic valve replacement on right ventricular-pulmonary artery coupling. *JACC Cardiovasc Interv*. 2019; **12**: 2145–2154.
48. Trejo-Velasco B, Estevez-Loureiro R, Carrasco-Chinchilla F, Fernandez-Vazquez F, Arzamendi D, Pan M, Pascual I, Nombela-Franco L, Amat-Santos IJ, Freixa X, Hernandez-Antolin RA, Trillo-Nouche R, Andraka Ikazuriaga L, Lopez-Minguez JR, Sanmiguel Cervera D, Sanchis J, Diez-Gil JL, Ruiz-Quevedo V, Urbano-Carrillo C, Becerra-Munoz VM, Benito-Gonzalez T, Li CH, Mesa D, Avanzas P, Armijo G, Serrador-Frutos AM, Sanchis L, Loban CF, Cid-Alvarez B, Hernandez-Garcia JM, Garrote-Coloma C, Fernandez-Peregrina E, Romero M, Leon Arguero V, Cruz-Gonzalez I. Prognostic role of TAPSE to PASP ratio in patients undergoing MitraClip procedure. *J Clin Med*. 2021; **10**: 1006.
49. Brener MI, Grayburn P, Lindenfeld J, Burkhoff D, Liu M, Zhou Z, Alu MC, Medvedofsky DA, Asch FM, Weissman NJ, Bax J, Abraham W, Mack MJ, Stone GW, Hahn RT. Right ventricular-pulmonary arterial coupling in patients with HF secondary MR: analysis from the COAPT trial. *JACC Cardiovasc Interv*. 2021; **14**: 2231–2242.
50. Fortuni F, Butcher SC, Dietz MF, van der Bijl P, Prihadi EA, De Ferrari GM, Ajmone Marsan N, Bax JJ, Delgado V. Right ventricular-pulmonary arterial coupling in secondary tricuspid regurgitation. *Am J Cardiol*. 2021; **148**: 138–145.
51. Nazario RA, Goldraich LA, Hastenteufel LCT, Santos ABS, Carrion L, Clausell N. Donor-recipient predicted heart mass ratio and right ventricular-pulmonary arterial coupling in heart transplant. *Eur J Cardiothorac Surg*. 2021; **59**: 847–854.
52. Schmeisser A, Rauwolf T, Groscheck T, Kropf S, Luani B, Tanev I, Hansen M, Meissler S, Steendijk P, Braun-Dullaeus RC. Pressure-volume loop validation of TAPSE/PASP for right ventricular arterial coupling in heart failure with pulmonary hypertension. *Eur Heart J Cardiovasc Imaging*. 2021; **22**: 168–176.
53. Forton K, Motoji Y, Caravita S, Faoro V, Naeije R. Exercise stress echocardiography of the pulmonary circulation and right ventricular-arterial coupling in healthy adolescents. *Eur Heart J Cardiovasc Imaging*. 2021; **22**: 688–694.
54. Suzuki M, Matsumoto K, Tanaka Y, Yamashita K, Shono A, Sumimoto K, Shibata N, Yokota S, Suto M, Dokuni K, Tanaka H, Otake H, Hirata KI. Preoperative coupling between right ventricle and pulmonary vasculature is an important determinant of residual symptoms after the closure of atrial septal defect. *Int J Cardiovasc Imaging*. 2021; **37**: 2931–2941.
55. Egbe AC, Miranda WR, Pellikka PA, Pislaru SV, Borlaug BA, Kothapalli S, Ananthaneni S, Sandhyavenu H, Najam M, Farouk Abdelsamid M, Connolly HM. Right ventricular and pulmonary vascular function indices for risk stratification of patients with pulmonary regurgitation. *Congenit Heart Dis*. 2019; **14**: 657–664.
56. Kim D, Park Y, Choi KH, Park TK, Lee JM, Cho YH, Choi JO, Jeon ES, Yang JH. Prognostic implication of RV coupling to pulmonary circulation for successful weaning from extracorporeal membrane oxygenation. *JACC Cardiovasc Imaging*. 2021; **14**: 1523–1531.
57. Bleakley C, Singh S, Garfield B, Morosin M, Surkova E, Mandalia MS, Dias B, Androulakis E, Price LC, McCabe C, Wort SJ, West C, Li W,

Khattar R, Senior R, Patel BV, Price S. Right ventricular dysfunction in critically ill COVID-19 ARDS. *Int J Cardiol*. 2021; **327**: 251–258.
58. Azpiri-Lopez JR, Galarza-Delgado DA, Colunga-Pedraza IJ, Arvizu-Rivera RI, Cardenas-de la Garza JA, Vera-Pineda R, Davila-Jimenez JA, Martinez-Flores CM, Rodriguez-Romero AB, Guajardo-Jauregui N. Echocardiographic evaluation of pulmonary hypertension, right ventricular function, and right ventricular-pulmonary arterial coupling in patients with rheumatoid arthritis. *Clin Rheumatol*. 2021; **40**: 2651–2656.
59. van Wezenbeek J, Groeneveldt JA, Llucia-Valldeperas A, van der Bruggen CE, Jansen SMA, Smits AJ, Smal R, van Leeuwen JW, Remedios CD, Keogh A, Humbert M, Dorfmuller P, Mercier O, Guignabert C, Niessen HWM, Handoko ML, Marcus JT, Meijboom LJ, Oosterveer FPT, Westerhof BE, Heijboer AC, Bogaard HJ, Vonk Noordegraaf A, Goumans MJ, de Man FS. Interplay of sex hormones and long-term right ventricular adaptation in a Dutch PAH-cohort. *J Heart Lung Transplant*. 2022; **41**: 445–457.
60. Brener MI, Lurz P, Hausleiter J, Rodes-Cabau J, Fam N, Kodali SK, Rommel KP, Muntane-Carol G, Gavazzoni M, Nazif TM, Pozzoli A, Alessandrini H, Latib A, Biasco L, Braun D, Brochet E, Denti P, Lubos E, Ludwig S, Kalbacher D, Estevez-Loureiro R, Connelly KA, Frerker C, Ho EC, Juliard JM, Harr C, Monivas V, Nickenig G, Pedrazzini G, Philippon F, Praz F, Puri R, Schofer J, Sievert H, Tang GHL, Andreas M, Thiele H, Unterhuber M, Himbert D, Alcazar MU, Von Bardeleben RS, Windecker S, Wild MG, Maisano F, Leon MB, Taramasso M, Hahn RT. Right ventricular-pulmonary arterial coupling and afterload reserve in patients undergoing transcatheter tricuspid valve repair. *J Am Coll Cardiol*. 2022; **79**: 448–461.
61. Boulate D, Amsallem M, Kuznetsova T, Zamanian RT, Fadel E, Mercier O, Haddad F. Echocardiographic evaluations of right ventriculo-arterial coupling in experimental and clinical pulmonary hypertension. *Physiol Rep*. 2019; **7**: e14322.
62. Cheng S, Li VW, So EK, Cheung YF. Right ventricular-pulmonary arterial coupling in repaired tetralogy of Fallot. *Pediatr Cardiol*. 2022; **43**: 207–217.
63. Li Y, Guo D, Gong J, Wang J, Huang Q, Yang S, Zhang X, Hu H, Jiang Z, Yang Y, Lu X. Right ventricular function and its coupling with pulmonary circulation in precapillary pulmonary hypertension: a three-dimensional echocardiographic study. *Front Cardiovasc Med*. 2021; **8**: 690606.
64. Addetia K, Muraru D, Badano LP, Lang RM. New directions in right ventricular assessment using 3-dimensional echocardiography. *JAMA Cardiol*. 2019; **4**: 936–944.
65. Lakatos B, Toser Z, Tokodi M, Doronina A, Kosztin A, Muraru D, Badano LP, Kovacs A, Merkely B. Quantification of the relative contribution of the different right ventricular wall motion components to right ventricular ejection fraction: the ReVISION method. *Cardiovasc Ultrasound*. 2017; **15**: 8.
66. Lang RM, Badano LP, Mor-Avi V, Afilalo J, Armstrong A, Ernande L, Flachskampf FA, Foster E, Goldstein SA, Kuznetsova T, Lancellotti P, Muraru D, Picard MH, Rietzschel ER, Rudski L, Spencer KT, Tsang W, Voigt JU. Recommendations for cardiac chamber quantification by echocardiography in adults: an update from the American Society of Echocardiography and the European Association of Cardiovascular Imaging. *J Am Soc Echocardiogr*. 2015; **28**: 1–39.e14.
67. Crean AM, Maredia N, Ballard G, Menezes R, Wharton G, Forster J, Greenwood JP, Thomson JD. 3D Echo systematically underestimates right ventricular volumes compared to cardiovascular magnetic resonance in adult congenital heart disease patients with moderate or severe RV dilatation. *J Cardiovasc Magn Reson*. 2011; **13**: 78.
68. Jone PN, Schafer M, Pan Z, Ivy DD. Right ventricular-arterial coupling ratio derived from 3-dimensional echocardiography predicts outcomes in pediatric pulmonary hypertension. *Circ Cardiovasc Imaging*. 2019; **12**: e008176.
69. Aubert R, Venner C, Huttin O, Haine D, Filippetti L, Guillaumot A, Mandry D, Marie PY, Juilliere Y, Chabot F, Chaouat A, Selton-Suty C. Three-dimensional echocardiography for the assessment of right ventriculo-arterial coupling. *J Am Soc Echocardiogr*. 2018; **31**: 905–915.
70. Trip P, Kind T, van de Veerdonk MC, Marcus JT, de Man FS, Westerhof N, Vonk-Noordegraaf A. Accurate assessment of load-independent right ventricular systolic function in patients with pulmonary hypertension. *J Heart Lung Transplant*. 2013; **32**: 50–55.
71. Nochioka K, Querejeta Roca G, Claggett B, Biering-Sorensen T, Matsushita K, Hung CL, Solomon SD, Kitzman D, Shah AM. Right ventricular function, right ventricular-pulmonary artery coupling, and heart failure risk in 4 US communities: the Atherosclerosis Risk in Communities (ARIC) study. *JAMA Cardiol*. 2018; **3**: 939–948.
72. Vijiiac A, Bataila V, Onciul S, Verinceanu V, Guzu C, Deaconu S, Petre I, Scarlatescu A, Zamfir D, Dorobantu M. Non-invasive right ventriculo-arterial coupling as a rehospitalization predictor in dilated cardiomyopathy: a comparison of five different methods. *Kardiol Pol*. 2022; **80**: 182–190.
73. Ishiwata J, Daimon M, Nakanishi K, Sugimoto T, Kawata T, Shinozaki T, Nakao T, Hirokawa M, Sawada N, Yoshida Y, Amiya E, Hatano M, Morita H, Yatomi Y, Komuro I. Combined evaluation of right ventricular function using echocardiography in non-ischaemic dilated cardiomyopathy. *ESC Heart Fail*. 2021; **8**: 3947–3956.
74. Kovacs A, Lakatos B, Tokodi M, Merkely B. Right ventricular mechanical pattern in health and disease: beyond longitudinal shortening. *Heart Fail Rev*. 2019; **24**: 511–520.
75. Surkova E, Kovacs A, Lakatos BK, Tokodi M, Fabian A, West C, Senior R, Li W. Contraction patterns of the systemic right ventricle: a three-dimensional echocardiography study. *Eur Heart J Cardiovasc Imaging*. 2021.
76. Surkova E, Kovacs A, Tokodi M, Lakatos BK, Merkely B, Muraru D, Ruocco A, Parati G, Badano LP. Contraction patterns of the right ventricle associated with different degrees of left ventricular systolic dysfunction. *Circ Cardiovasc Imaging*. 2021; **14**: e012774.
77. Marcus JT, Gan CT, Zwanenburg JJ, Boonstra A, Allaart CP, Gotte MJ, Vonk-Noordegraaf A. Interventricular mechanical asynchrony in pulmonary arterial hypertension: left-to-right delay in peak shortening is related to right ventricular overload and left ventricular underfilling. *J Am Coll Cardiol*. 2008; **51**: 750–757.
78. Lumens J, Arts T, Marcus JT, Vonk-Noordegraaf A, Delhaas T. Early-diastolic left ventricular lengthening implies pulmonary hypertension-induced right ventricular decompensation. *Cardiovasc Res*. 2012; **96**: 286–295.
79. Badagliacca R, Pezzuto B, Papa S, Poscia R, Manzi G, Pascaretta A, Miotti C, Luongo F, Scoccia G, Ciciarello F, Casu G, Sciomer S, Fedele F, Naeije R, Vizza CD. Right ventricular strain curve morphology and outcome in idiopathic pulmonary arterial hypertension. *JACC Cardiovasc Imaging*. 2021; **14**: 162–172.
80. Vonk Noordegraaf A, Westerhof BE, Westerhof N. The relationship between the right ventricle and its load in pulmonary hypertension. *J Am Coll Cardiol*. 2017; **69**: 236–243.
81. Russell K, Eriksen M, Aaberge L, Wilhelmsen N, Skulstad H, Remme EW, Haugaa KH, Opdahl A, Fjeld JG, Gjesdal O, Edvardsen T, Smiseth OA. A novel clinical method for quantification of regional left ventricular pressure-strain loop area: a non-invasive index of myocardial work. *Eur Heart J*. 2012; **33**: 724–733.
82. Butcher SC, Feloukidis C, Kamperidis V, Yedidya I, Stassen J, Fortuni F, Vrana E, Mouratoglou SA, Boutou A, Giannakoulas G, Playford D, Ajmone Marsan N, Bax JJ, Delgado V. Right

ventricular myocardial work characterization in patients with pulmonary hypertension and relation to invasive hemodynamic parameters and outcomes. *Am J Cardiol*. 2022; **177**: 151–161.
83. Butcher SC, Fortuni F, Montero-Cabezas JM, Abou R, El Mahdiui M, van der Bijl P, van der Velde ET, Ajmone Marsan N, Bax JJ, Delgado V. Right ventricular myocardial work: proof-of-concept for non-invasive assessment of right ventricular function. *Eur Heart J Cardiovasc Imaging*. 2021; **22**: 142–152.
84. Sade LE, Colak A, Duzgun SA, Hazirolan T, Sezgin A, Donal E, Butcher SC, Ozdemir H, Pirat B, Eroglu S, Muderrisoglu H. Approach to optimal assessment of right ventricular remodelling in heart transplant recipients: insights from myocardial work index, T1 mapping, and endomyocardial biopsy. *Eur Heart J Cardiovasc Imaging*. 2022.
85. Ren X, Johns RA, Gao WD. Right heart in pulmonary hypertension: from adaptation to failure. *Pulm Circ*. 2019; **9**: 2045894019845611.
86. Vonk-Noordegraaf A, Haddad F, Chin KM, Forfia PR, Kawut SM, Lumens J, Naeije R, Newman J, Oudiz RJ, Provencher S, Torbicki A, Voelkel NF, Hassoun PM. Right heart adaptation to pulmonary arterial hypertension: physiology and pathobiology. *J Am Coll Cardiol*. 2013; **62**: D22–D33.
87. Dutta T, Aronow WS. Echocardiographic evaluation of the right ventricle: clinical implications. *Clin Cardiol*. 2017; **40**: 542–548.
88. Focardi M, Cameli M, Carbone SF, Massoni A, De Vito R, Lisi M, Mondillo S. Traditional and innovative echocardiographic parameters for the analysis of right ventricular performance in comparison with cardiac magnetic resonance. *Eur Heart J Cardiovasc Imaging*. 2015; **16**: 47–52.
89. Motoji Y, Tanaka H, Fukuda Y, Ryo K, Emoto N, Kawai H, Hirata K. Efficacy of right ventricular free-wall longitudinal speckle-tracking strain for predicting long-term outcome in patients with pulmonary hypertension. *Circ J*. 2013; **77**: 756–763.
90. Badano LP, Muraru D, Parati G, Haugaa K, Voigt JU. How to do right ventricular strain. *Eur Heart J Cardiovasc Imaging*. 2020; **21**: 825–827.
91. Vonk Noordegraaf A, Haddad F, Bogaard HJ, Hassoun PM. Noninvasive imaging in the assessment of the cardiopulmonary vascular unit. *Circulation*. 2015; **131**: 899–913.
92. Greiner S, Jud A, Aurich M, Hess A, Hilbel T, Hardt S, Katus HA, Mereles D. Reliability of noninvasive assessment of systolic pulmonary artery pressure by Doppler echocardiography compared to right heart catheterization: analysis in a large patient population. *J Am Heart Assoc*. 2014; **3**: e001103.
93. D'Alto M, Romeo E, Argiento P, D'Andrea A, Vanderpool R, Correra A, Bossone E, Sarubbi B, Calabro R, Russo MG, Naeije R. Accuracy and precision of echocardiography versus right heart catheterization for the assessment of pulmonary hypertension. *Int J Cardiol*. 2013; **168**: 4058–4062.
94. Rich JD, Shah SJ, Swamy RS, Kamp A, Rich S. Inaccuracy of Doppler echocardiographic estimates of pulmonary artery pressures in patients with pulmonary hypertension: implications for clinical practice. *Chest*. 2011; **139**: 988–993.
95. Sade LE, Katz WE. Right ventricle deserves more attention in transcutaneous aortic valve replacement patients. *J Card Fail*. 2021; **27**: 1345–1347.
96. Ghio S, Klersy C, Magrini G, D'Armini AM, Scelsi L, Raineri C, Pasotti M, Serio A, Campana C, Vigano M. Prognostic relevance of the echocardiographic assessment of right ventricular function in patients with idiopathic pulmonary arterial hypertension. *Int J Cardiol*. 2010; **140**: 272–278.
97. Ozpelit E, Akdeniz B, Ozpelit EM, Tas S, Alpaslan E, Bozkurt S, Arslan A, Badak O. Impact of severe tricuspid regurgitation on accuracy of echocardiographic pulmonary artery systolic pressure estimation. *Echocardiography*. 2015; **32**: 1483–1490.
98. Humbert M, Kovacs G, Hoeper MM, Badagliacca R, Berger RMF, Brida M, Carlsen J, Coats AJS, Escribano-Subias P, Ferrari P, Ferreira DS, Ghofrani HA, Giannakoulas G, Kiely DG, Mayer E, Meszaros G, Nagavci B, Olsson KM, Pepke-Zaba J, Quint JK, Radegran G, Simonneau G, Sitbon O, Tonia T, Toshner M, Vachiery JL, Vonk Noordegraaf A, Delcroix M, Rosenkranz S, Group EESD. 2022 ESC/ERS Guidelines for the diagnosis and treatment of pulmonary hypertension. *Eur Respir J*. 2022; **in press**: 2200879.
99. Kind T, Mauritz GJ, Marcus JT, van de Veerdonk M, Westerhof N, Vonk-Noordegraaf A. Right ventricular ejection fraction is better reflected by transverse rather than longitudinal wall motion in pulmonary hypertension. *J Cardiovasc Magn Reson*. 2010; **12**: 35.
100. Wessels JN, Mouratoglou SA, van Wezenbeek J, Handoko ML, Marcus JT, Meijboom LJ, Westerhof BE, Bogaard HJ, Strijkers GJ, Vonk Noordegraaf A, de Man FS. Right atrial function is associated with right venticular diastolic stiffness: RA-RV interaction in pulmonary arterial hypertension. *Eur Respir J*. 2022; **59**: 2101454.
101. van Wezenbeek J, Kianzad A, van de Bovenkamp A, Wessels J, Mouratoglou SA, Braams NJ, Jansen SMA, Meulblok E, Meijboom LJ, Marcus JT, Vonk Noordegraaf A, Jose Goumans M, Jan Bogaard H, Handoko ML, de Man FS. Right ventricular and right atrial function are less compromised in pulmonary hypertension secondary to heart failure with preserved ejection fraction: a comparison with pulmonary arterial hypertension with similar pressure overload. *Circ Heart Fail*. 2022; **15**: e008726.